Self-Aggregation of Amino-Acidate Half-Sandwich Ruthenium(II) Complexes in Solution: From Monomers to Nanoaggregates

Gianluca Ciancaleoni, Ilona Di Maio, Daniele Zuccaccia, and Alceo Macchioni*

Dipartimento di Chimica, Università di Perugia, via Elce di Sotto, 8, 06123 Perugia, Italy

Received October 3, 2006

The aggregation tendency of [RuCl(AA)(Arene)] complexes (**1**, AA = amino acidate = Gly, Arene = *p*-cymene; **2**, AA = Ala, Arene = *p*-cymene; **3**, AA = *N*,*N*′-dimethyl-Gly, Arene = benzene; **3b**, AA = *N*,*N*′-dimethyl-Gly, Arene = *p*-cymene; **3c**, AA = *N*,*N*′-dimethyl-Gly, Arene = hexamethylbenzene; **4a**, AA = *t*-Leu, Arene = benzene; **4b**, AA = *t*-Leu, Arene = *p*-cymene; **4c**, AA = *t*-Leu, Arene = hexamethylbenzene; **5**, AA = α,α′-Me_2-Gly, Arene = *p*-cymene; **6**, AA = α,α′-Ph_2-Gly, Arene = *p*-cymene; **7**, AA = Pro, Arene = *p*-cymene) as a function of the concentration and solvent ($CDCl_3$, CD_2Cl_2, acetone-d_6, and 2-propanol-d_8) was investigated through diffusion NMR measurements. The equilibrium constant (K) and the standard variation of the free energy (ΔG°) for the aggregation process were determined by applying the Equal K self-aggregation model. The highest level of aggregation was observed for complexes **1**, **2**, and **4**, bearing the NH_2 moiety, which was involved in intermolecular H-bonding. Complex **2** formed aggregates with a hydrodynamic radius (r_H) equal to 20.8 Å in $CDCl_3$ ($\Delta G^\circ_{296K} = -7.1 \pm 0.7$ kcal mol^{-1}) at a concentration of 124.9 mM, corresponding to an aggregation number (N) of 133. On the other hand, complex **3c** did not show any tendency to aggregate ($N = 1.1$, 0.5 mM in $CDCl_3$). The aggregation tendency decreased as the steric hindrance of arene (**4a** > **4b** > **4c**) and AA (**1** ≈ **2** > **5** ≈ **4b** > **6**) and the polarity and proticity of the solvent increased. For complex **2**, $-\Delta G^\circ$(kcal/mol) was 7.1 in $CDCl_3$ ($\epsilon_r = 4.81$) > 5.6 in CD_2Cl_2 ($\epsilon_r = 8.93$) > 3.9 in acetone-d_6 ($\epsilon_r = 20.56$) > 3.0 in 2-propanol-d_8 ($\epsilon_r = 19.92$). While the two diastereoisomers of complexes **2** and **4b** showed substantially the same tendency to self-aggregate, diastereoisomer (R_{Ru}, S_N, S_C)-**7** showed a remarkably higher aggregation tendency than the other one [(S_{Ru}, S_N, S_C)-**7**] throughout the entire concentration range (1.4−178.0 mM) in $CDCl_3$, indicating that a diastereoselective recognition process is occurring in solution [$|\Delta(\Delta G^\circ_{296K})| = 1.8 \pm 0.5$ kcal mol^{-1}].

Introduction

Noncovalent interactions occurring in the second coordination sphere of transition-metal complexes may profoundly alter their structure and reactivity. This is well-recognized for ionic compounds[1] and is also becoming evident for neutral ones. In fact, interactions in the second coordination sphere have been exploited to optimize the recognition process between the substrate and the catalyst[2] and to impart or improve the enantioselectivity of the catalyst itself.[3] It has also been proposed[4,5] that they may be solely responsible for the activation process without the necessity of substrate−metal interactions in analogy with enzymatic and organo catalysis.

The presence of functionalities suitable for undergoing intermolecular noncovalent interactions, in the second coordination sphere, may also lead to self-aggregation of transition-metal complexes.[6,7] In our opinion, this aspect has been underestimated given that it can have important consequences on the reactivity.

Recently, we reported preliminary results[7] concerning the remarkable tendency to self-aggregate of Noyori[5] and amino acidate[8,9] half-sandwich ruthenium(II) complexes in both aprotic solvents with low relative permittivity and protic solvents with medium to high relative permittivity, including 2-propanol, which is the solvent used in transfer hydrogenation. This is particularly interesting since these catalysts are supposed to carry out the activation process in the second coordination sphere through a bifunctional mechanism.[10] From our results it cannot be excluded that the catalysis is carried out by a noncovalent dimeric species.

Here we report in full the results of a systematic PGSE (pulsed field gradient spin−echo)[11] NMR investigation on the self-aggregation tendency of [RuCl(AA)(Arene)] compounds. The nature of arene and amino acidate ligands and solvent has

* Corresponding author. E-mail: alceo@unipg.it. Fax: +39 075 5855598. Phone: +39 075 5855579.

(1) Macchioni, A. *Chem. Rev.* **2005**, *105*, 2039.

(2) Das, S.; Incarvito, C. D.; Crabtree, R. H.; Brudvig, G. W. *Science* **2006**, *312*, 1941.

(3) Thomas, C. M.; Ward, T. R. *Chem. Soc. Rev.* **2005**, *34*, *337*. Krämer, R. *Angew. Chem., Int. Ed.* **2006**, *45*, *858*. Roelfes, G.; Feringa, B. L. *Angew. Chem., Int. Ed.* **2005**, *44*, 3230.

(4) Shvo, Y.; Czarkie, D.; Rahamim, Y.; Chodash, D. F. *J. Am. Chem. Soc.* **1986**, *108*, *7400*. Menashe, N.; Shvo, Y. *Organometallics* **1991**, *10*, 3885.

(5) Noyori, R.; Hashiguchi, S. *Acc. Chem. Res.* **1997**, *30*, *97*. Yamakawa, M.; Ito, H.; Noyori, R. *J. Am. Chem. Soc.* **2000**, *122*, *1446*. Noyori, R.; Yamakawa, M.; Hashiguchi, S. *J. Org. Chem.* **2001**, *66*, 7931.

(6) Burini, A.; Fackler, J. P., Jr.; Galassi, R.; Macchioni, A.; Omary, M. A.; Rawashdeh-Omary, M. A.; Pietroni, B. R.; Sabatini, S.; Zuccaccia, C. *J. Am. Chem. Soc.* **2002**, *124*, 4570. Macchioni, A.; Romani, A.; Zuccaccia, C.; Guglielmetti, G.; Querci, C. *Organometallics* **2003**, *22*, 1526. Zuccaccia D.; Sabatini S.; Bellachioma G.; Cardaci G.; Clot, E.; Macchioni A. *Inorg. Chem.* **2003**, *42*, 5465. Zuccaccia, C.; Stahl, N. G.; Macchioni, A.; Chen, M.-C.; Roberts, J. A.; Marks, T. J. *J. Am. Chem. Soc.* **2004**, *126*, 1448. Zuccaccia, D.; Bellachioma, G.; Cardaci, G.; Zuccaccia, C.; Macchioni, A. *Dalton Trans.* **2006**, 1963.

(7) Zuccaccia, D.; Clot, E.; Macchioni, A. *New J. Chem.* **2005**, *29*, 430−433.

(8) Severin, K.; Bergs, R.; Beck, W. *Angew. Chem., Int. Ed.* **1998**, *37*, 1635.

(9) Ohta, T.; Nakahara, S.-I.; Shigemura, Y.; Hattori, K.; Furukawa, I. *Chem. Lett.* **1998**, *6*, 491. Kathó, Á.; Carmona, D.; Viguri, F.; Remacha, C. D.; Kovács, J.; Joó, F.; Oro, L. A. *J. Organomet. Chem.* **2000**, *593*−594, 299.

10.1021/om060904e CCC: $37.00
Publication on Web 01/04/2007

Scheme 1

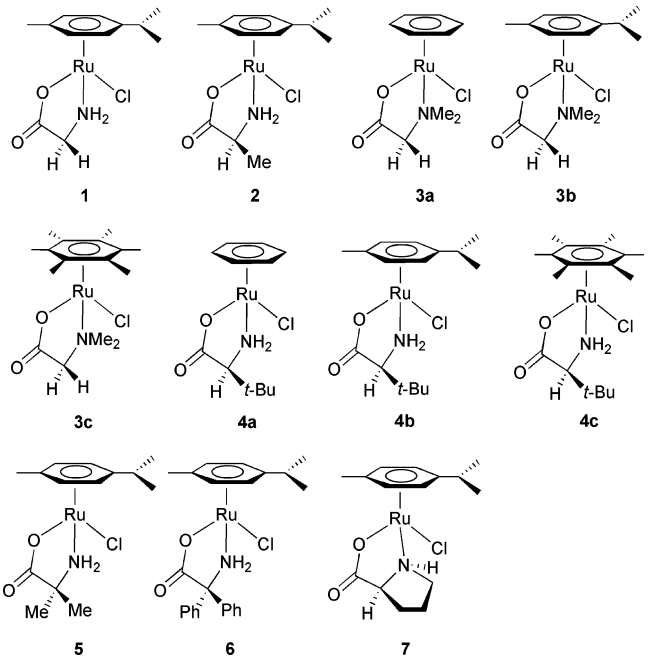

been varied in order to identify and quantify the noncovalent interactions that are responsible for the self-aggregation. Nanoaggregates have been observed in solvents with low relative permittivity at elevated concentration mainly due to the establishment of a network of hydrogen bonds. Extended self-aggregation has seldom been observed in organic compounds,[12−14] and the results presented here are a novelty for transition-metal complexes.[15]

Results and Discussion

Synthesis. Complexes **1**−**7** (Scheme 1) were synthesized by the reaction of a suitable amino acid with an appropriate $[Ru_2(\eta^6\text{-arene})_2Cl_2(\mu\text{-Cl})_2]$ dimer in MeOH in the presence of an equivalent of *t*-BuOK. Starting from the (S_C)-enantiopure amino acid the two diastereoisomers (S_{Ru}, S_C) and (R_{Ru}, S_C), respectively, were obtained for complexes **2** and **4** due to the chirality on the metal center.[16] In the case of the reaction with (S_C)-proline, due to the presence of another stereogenic center, i.e., the nitrogen atom that always adopts the same configuration as the asymmetric carbon of the amino acidate ligand,[17] the two diastereoisomers (S_{Ru}, S_N, S_C)-**7** and (R_{Ru}, S_N, S_C)-**7**, respectively, were obtained.

The equilibrium ratio of the two diasteroisomers depended on the ligand. The (*S*)-configuration at the metal was adopted by the major component of the mixtures, in all cases.[17] This was verified for complex **7** since the chemical shift of the N−H proton is a good indicator of its orientation.[18] In fact, when N−H points toward the cymene, it resonates about 2−3 ppm at higher frequency with respect to when it is directed toward the chloride.

PGSE NMR Measurements. The tendency of complexes **1**−**7** to self-aggregate in solution was investigated by means of PGSE NMR diffusion measurements. Extensive investigations were carried out for complex **2**, which showed the highest aggregation tendency, comparable only to that of the analogue with glycine **1**, which, on the other hand, did not dissolve in most organic solvents. PGSE NMR measurements were then carried out on the other complexes where the arene and amino acidate ligands were varied with the aim of selectively turning on and off the intermolecular interactions that were supposed to be responsible for the aggregation and, consequently, allowing them to be identified and quantified.

Using the PGSE NMR measurements, the translational self-diffusion coefficient (D_t) of the species present in solution was determined. The latter allowed the hydrodynamic radius (r_H) of the diffusing species to be evaluated by taking advantage of the Stokes−Einstein equation, eq 1:

$$D_t = \frac{kT}{c\pi\eta r_H} \tag{1}$$

where k is the Boltzmann constant, T is the temperature, c is a numerical factor, and η is the solution viscosity. The c factor substantially depends on the size of the diffusing species; the correct evaluation is particularly critical for medium- and small-sized molecules, for which c differs significantly from both 4 (slip boundary condition) and 6 (stick boundary conditions) and when a large variation of the average dimensions for a given solute occurs on changing either solvent or concentration.[18] This is exactly the case reported here (Supporting Information), in that complexes passed from mononuclear species to nanoaggregates depending on the ligands, solvent, and concentration (*vide infra*). The hydrodynamic volume (V_H) of the aggregates was determined by r_H assuming that they had a spherical shape. Finally, the aggregation number (N), defined as the ratio of experimental hydrodynamic volume and the van der Waals volume (V_{vdW}), was derived in order to estimate the average nuclearity of the noncovalent adduct. For large aggregates ($V_H > 3V_{vdW}$), N was calculated by the $[(V_H - V_{INT})/V_{vdW}]$ ratio,

(10) Clapham, S. E.; Hadzovic, A.; Morris, R. H. *Coord. Chem. Rev.* **2004**, *248*, 2201. Muñiz, K. *Angew. Chem., Int. Ed.* **2005**, *44*, 6622. Samec, J. S. M.; Bäckvall, J.-E.; Andersson, P. G.; Brandt, P. *Chem. Soc. Rev.* **2006**, *35*, 237.

(11) Hahn, E. L. *Phys. Rev.* **1950**, *80*, *580*−594. Stejskal, E. O; Tanner, J. E. *J. Chem. Phys.* **1965**, *42*, 288. Stilbs, P. *Prog. Nucl. Magn. Reson. Spectrosc.* **1987**, *19*, 1. Price, W. S. *Concepts Magn. Reson.* **1997**, *9*, 299. Price, W. S. *Concepts Magn. Reson.* **1998**, *10*, 197. Johnson, C. S., Jr. *Prog. Nucl. Magn. Reson. Spectrosc.* **1999**, *34*, 203. Valentini, M.; Rüegger, H.; Pregosin, P. S. *Helv. Chim. Acta* **2001**, *84*, 2833. Binotti, B.; Macchioni, A.; Zuccaccia, C.; Zuccaccia, D. *Comments Inorg. Chem.* **2002**, *23*, 417. Macchioni, A. In *Perspectives in Organometallic Chemistry*; Screttas, C. G., Steele B. R., Eds.; The Royal Society of Chemistry: Cambridge, 2003; pp 196−207. Pregosin, P. S.; Martinez-Viviente, E.; Kumar, P. G. A. *Dalton Trans*. **2003**, 4007. Bagno, A.; Rastrelli, F.; Saielli, G. *Prog. Nucl. Magn. Reson. Spectrosc.* **2005**, *47*, 41. Brand, T.; Cabrita, E. J.; Berger, S. *Prog. Nucl. Magn. Reson. Spectrosc.* **2005**, *46*, 159. Cohen, Y.; Avram, L.; Frish, L. *Angew. Chem., Int. Ed.* **2005**, *44*, 520−554. Pregosin, P. S.; Kumar, P. G. A.; Fernández, I. *Chem. Rev.* **2005**, *105*, 2977.

(12) Kunimura, M.; Sakamoto, S.; Yamaguchi, K. *Org. Lett.* **2002**, *4* (3), 347−350.

(13) (a) Jadzin, J.; Stockhausen, M.; Zywucki, B. *J. Phys. Chem.* **1987**, *91*, 754. (b) Ohta, T.; Nakahara, Y. S.; Hattori, K.; Furukawa, I. *Chem. Lett.* **1998**, *6*, 491.

(14) Geringer M.; Gruber, H.; Sterk, H. *J. Phys. Chem.* **1991**, *95*, 2525.

(15) For self-aggregation of Ru surfactants: Bowers, J.; Danks, M. J.; Duncan, W.; Heenan, R. K. *Langmuir* **2003**, *19*, *292*. Bowers, J.; Amos, K. E.; Duncan, W.; Heenan, R. K. *Langmuir* **2005**, *21*, 5696. Domýnguez-Gutierrez, D.; Surtchev, M.; Eiser, E.; Elsevier, C. J. *Nano Lett.* **2006**, *6*, 145.

(16) Brunner, H.; Henning, F.; Zabel, M. *Z. Anorg. Allg. Chem.* **2004**, *630*, 91, and references therein. Brunner, H.; Zwack, T.; Zabel, M.; Beck, W.; Boehm, A. *Organometallics* **2003**, *22*, 1741, and references therein. Brunner, H.; Henning, F.; Weber, M.; Zabel, M.; Carmona, D.; Lahoz, F. J. *Synthesis* **2003**, 1091. For a review: Brunner, H. *Angew. Chem., Int. Ed.* **1999**, *38*, 1194. Brunner, H. *Eur. J. Inorg. Chem.* **2001**, 905.

(17) (a) Carmona, D.; Vega, C.; Lahoz, F. J.; Atencio, R.; Oro, L. A. *Organometallics* **2000**, *19*, 2273. (b) Carmona, D.; Lahoz, F. J.; Atencio, R.; Oro, L. A.; Lamata, M. P.; Viguri, F.; San, Jose, E.; Vega, C.; Reyes, J.; Joo, F.; Katho, A. *Chem.−Eur. J.* **1999**, *5*, 1544. (c) Carmona, D.; Mendoza, A.; Lahoz, F. J.; Oro, L. A., *J. Organomet. Chem.* **1990**, *396*, C17. (d) Carmona, D.; Lamata, M. P.; Oro, L. A., *Eur. J. Inorg. Chem.*, **2002**, 2239.

(18) Zuccaccia, D.; Macchioni, A. *Organometallics* **2005**, *24*, 3476.

Table 1. Diffusion Coefficients (D_t, $m^2\ s^{-1}$), Hydrodynamic Radius (r_H, Å), Hydrodynamic Volume (V_H, $Å^3$), Aggregation Number (N), and Concentration (C, mM) for Compounds (S_{Ru},S_C)-2 and (R_{Ru},S_C)-2 in Different Solvents (ϵ_r at 25 °C)

entry	solvent	$10^{10}\ D_t$	r_H	V_H	N	C
		(S_{Ru}, S_C)-**2**				
1	$CDCl_3$ (4.81[a])	7.95	5.5	686	2.9	0.3
2	$CDCl_3$ (4.81[a])	5.12	7.7	1927	7.8	1.7
3	$CDCl_3$ (4.81[a])	3.38	11.1	5713	21.6	5.7
4	$CDCl_3$ (4.81[a])	2.93	12.8	8702	32.3	11.1
5	$CDCl_3$ (4.81[a])	2.07	16.2	17 908	64.2	39.3
6	$CDCl_3$ (4.81[a])	1.46	20.8	37 858	133.0	124.9
7	CD_2Cl_2 (8.93)	12.4	4.7	445	1.9	0.09
8	CD_2Cl_2 (8.93)	8.67	6.0	883	3.7	3.9
9	CD_2Cl_2 (8.93)	6.69	7.5	1757	7.2	10.1
10	CD_2Cl_2 (8.93)	4.89	9.8	3906	15.0	27.7
11	CD_2Cl_2 (8.93)	4.43	10.4	4690	17.9	40.2
12	CD_2Cl_2 (8.93)	3.04	13.0	9288	37.4	106
13	CD_2Cl_2 (8.93)	2.43	14.7	13 387	48.6	165
14	acetone-d_6 (20.56)	15.9	5.2	601	2.5	0.5
15	acetone-d_6 (20.56)	16.9	5.5	701	3.0	1.3
16	acetone-d_6 (20.56)	14.9	5.4	686	2.9	1.4
17	acetone-d_6 (20.56)	14.4	5.5	713	3.0	3.4
18	acetone-d_6 (20.56)	10.7	6.3	1047	4.3	14.0
19	acetone-d_6 (20.56)	10.7	7.0	1408	5.8	28[b]
20	2-propanol-d_8 (19.92)	1.85	5.4	667	2.8	4.8
21	2-propanol-d_8 (19.92)	1.62	5.8	830	3.5	26
22	2-propanol-d_8 (19.92)	1.52	5.9	873	3.7	36
		($R_{Ru'}$ S_C)-**2**				
23	$CDCl_3$ (4.81[a])	8.18	5.4	645	2.7	0.2
24	$CDCl_3$ (4.81[a])	5.49	7.3	1596	5.0	1.3
25	$CDCl_3$ (4.81[a])	3.84	9.9	4003	15.3	3.3
26	$CDCl_3$ (4.81[a])	3.30	11.4	6206	23.4	5.9
27	$CDCl_3$ (4.81[a])	2.14	15.8	16 397	59.0	20.7
28	$CDCl_3$ (4.81[a])	1.53	20.0	33 510	118.0	65.1
29	CD_2Cl_2 (8.93)	12.7	4.6	418	1.8	0.08
30	CD_2Cl_2 (8.93)	9.39	5.6	723	3.1	2.8
31	CD_2Cl_2 (8.93)	7.40	6.8	1340	5.5	8.5
32	CD_2Cl_2 (8.93)	5.44	8.8	2887	11.3	20.0
33	CD_2Cl_2 (8.93)	4.86	9.5	3599	13.9	25.1
34	CD_2Cl_2 (8.93)	3.23	12.3	7808	29.1	61.5
35	CD_2Cl_2 (8.93)	2.54	14.1	11 767	43.1	104
36	acetone-d_6 (20.56)	16.5	5.1	546	2.3	0.2
37	acetone-d_6 (20.56)	18.0	5.3	605	2.6	0.7
38	acetone-d_6 (20.56)	15.2	5.4	645	2.7	1.1
39	acetone-d_6 (20.56)	14.6	5.5	689	2.9	2.2
40	acetone-d_6 (20.56)	18.0	5.8	826	3.5	7.2
41	acetone-d_6 (20.56)	11.1	6.7	1267	5.2	26[b]
42	2-propanol-d_8 (19.92)	1.93	5.3	606	2.6	4.2
43	2-propanol-d_8 (19.92)	1.60	5.9	856	3.6	24
44	2-propanol-d_8 (19.92)	1.55	5.9	843	3.5	34

[a] ϵ_r at 20 °C. [b] Saturated solution.

where V_{INT} represents the interstitial volume. The latter was roughly estimated as described in the Experimental Section assuming a face-centered cubic package of the monomers.

(a) Aggregation of Complex 2 as a Function of Solvent and Concentration. ^{1}H-PGSE NMR data for the two diastereoisomers (S_{Ru}, S_C)-**2** and (R_{Ru}, S_C)-**2** are reported in Table 1. The trends of N as a function of the concentration in different solvents are illustrated in Figure 1. The two diastereoisomers showed a similar and marked tendency to self-aggregate (Figure 1) that increased by increasing the concentration and decreasing the relative permittivity (ϵ_r) of the solvents. In $CDCl_3$ at the highest concentration investigated, complex (S_{Ru}, S_C)-**2** afforded an aggregate with $r_H = 20.8$ Å and an aggregation number of 133 (Table 1, entry 6). Even at the lowest concentration investigated, dimers or trimers were prevalently present (entries 1, 7, 14, 20, 23, 29, 36, and 42 in Table 1).

The level of aggregation at the same concentration was reduced by about a third passing from $CDCl_3$ ($\epsilon_r = 4.81$) to CD_2Cl_2 ($\epsilon_r = 8.93$) and by about a tenth passing from $CDCl_3$ ($\epsilon_r = 4.81$) to acetone-d_6 ($\epsilon_r = 20.56$) (Figure 1). The level of aggregation also depended on the nature of the solvent: comparing the data for acetone-d_6 with those of 2-propanol-d_8, which has about the same dielectric constant, it is clear that the protic nature of the solvent decreases the tendency of the ruthenium complexes to self-aggregate (Figure 1).

The significant tendency of complex **2** to aggregate can be rationalized considering that it can undergo several noncovalent interactions. H-bond (HB) acceptors (chlorine atom and oxygen atoms of the carboxylate groups), an HB donor (amino group), and carbon atoms with a partial positive charge (aromatic C−H, aliphatic C−H in α-position with respect to the carboxylate group) are present in **2**. Consequently, classical hydrogen bonding and C−H···X interactions[19] can be established. In addition, the arene ligand can be involved in $\pi-\pi$ stacking interactions. All these interactions have been observed in the solid state of complexes [RuCl(*S*-Ala)(Arene)] (Arene = mesitylene[20] or benzene[21]). The case of [RuCl(*S*-Ala)(mesitylene)], which differs from **2** in that it has a mesitylene ligand in place of cymene, is shown in Figure 2.

Every Ru unit is surrounded by four other units and undergoes NH_2···Cl (distance N···Cl = 3.34 Å) and NH_2···O═CO (distance N···O = 2.96 Å) *hydrogen bonding*, CH···Cl and CH···O interactions[19] (distance C_{arene}···Cl = 3.79 Å), and $\pi-\pi$ *stacking* between two arene moieties (mean slip angle between the normal of one arene plane and the centroid vector = 15° and centroid to centroid distance = 3.63 Å).[22] The three-dimensional repetition of all these interactions affords a network that determines the supramolecular structure of these complexes. The marked tendency of complex **2** to aggregate can be justified by assuming that the above-mentioned intermolecular interactions observed for [RuCl(*S*-Ala)(Arene)] complexes in the solid state also occur in solution.

(b) Aggregation of Complexes 3−7. ^{1}H-PGSE NMR measurements were carried out for complexes **3**−**7** in order to establish the relative importance of the three noncovalent interactions described above. The results are shown in Table 2 (see Supporting Information for a complete list of the ^{1}H-PGSE NMR experiments). Before discussing in detail the effect of ligand variation on the aggregation tendency of the complexes, it is extremely important to note that the N value for complex **3c** in $CDCl_3$ (Table 2) and CD_2Cl_2 (Supporting Information) was 1.1 and 1.0, respectively. Therefore, it is exclusively present as a monomer. Due to the absence of N−H HB donors and positively polarized aromatic C−Hs and to the presence of six methyl groups in the arene that hinder the $\pi-\pi$ interaction, only the interactions between CH_2 and Cl or O could occur in **3c**. Evidently, the latter interactions alone could not afford significant aggregation. From a methodological point of view, the fact that the aggregation number in **3c** is equal to 1 indicates that the hydrodynamic volume is a good descriptor of the van der Waals volume for this class of compounds, ensuring that the PGSE NMR measurements are accurate.

From the data reported in Table 2, it is clear that H-bonding is the main aggregation motif between those illustrated in Figure

(19) (a) Brunner, H.; Weber, M.; Zabel, M.; Zwack, T. *Angew. Chem., Int. Ed.* **2003**, *42*, 1859. (b) Brunner, H.; Weber, M.; Zabel, M. *Coord. Chem. Rev.* **2003**, *242*, 3.

(20) Carter, L. C.; Davies, D. L.; Duffy, K. T.; Fawcett, J.; Russell, D. R. *Acta Crystallogr., Sect. C* **1994**, *C50*, 1559.

(21) Sheldrick, W. S.; Heeb, S. *Inorg Chim. Acta* **1990**, *168*, 93.

(22) For hydrogen bond parameters see: (a) Steiner, T. *Angew. Chem., Int. Ed.* **2002**, *41*, 48. (b) Jeffrey, G. A. *An Introduction to Hydrogen Bonding*; Oxford University Press: Oxford, 1997. For hydrogen bonds with good metal-bonded halogen acceptors see: (c) Yap, G.; Rheingold, A. L.; Das, P.; Crabtree, R. H. *Inorg. Chem.* **1995**, *34*, 3476. For $\pi-\pi$ stacking parameters see: (d) Janiak, C. J. *J. Chem. Soc., Dalton Trans.* **2000**, 3885. Hunter, C. A.; Sanders, J. K. *J. Am. Chem. Soc.* **1990**, *112*, 5525.

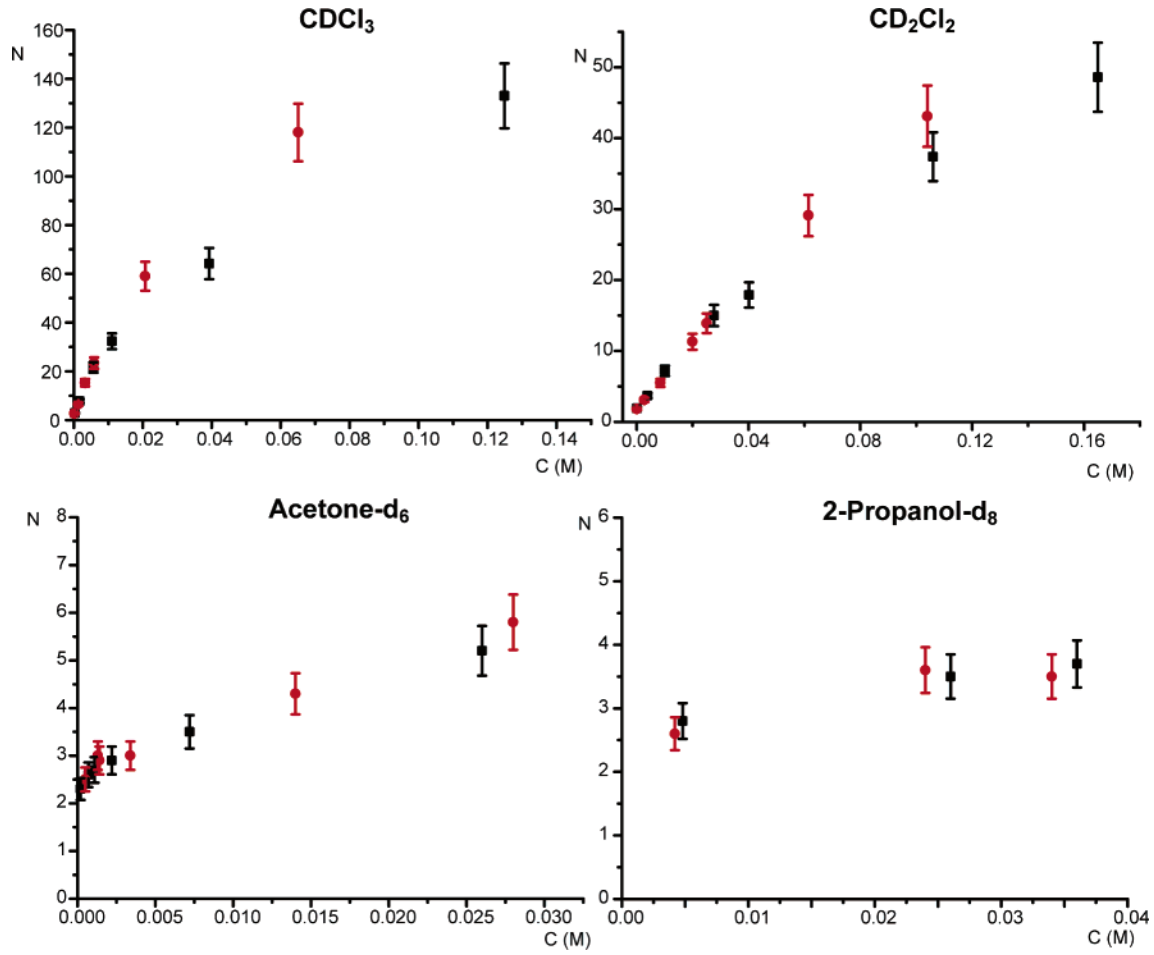

Figure 1. Dependence of the aggregation number (N) on the concentration of complex **2** [■ (S_{Ru}, S_C)-**2**, ● (R_{Ru}, S_C)-**2**] in different solvents.

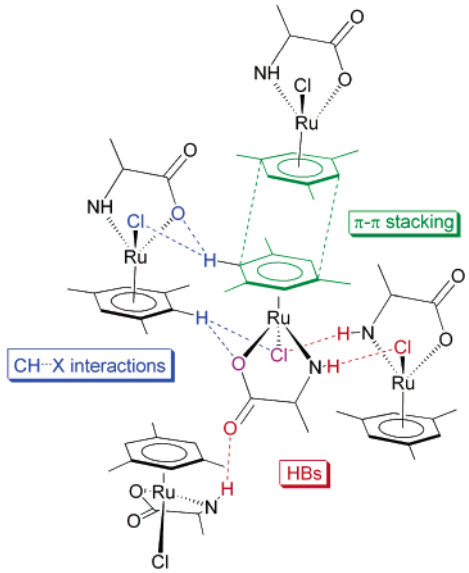

Figure 2. Noncovalent interactions present in the X-ray single-crystal structure of RuCl(*S*-Ala)(Mes) reported by Carter et al.[20]

2. The highest level of aggregation was observed for complexes **1**, **2**, and **4**, all bearing the NH_2 moiety. Nevertheless, steric effects play an important role in modulating the establishment of HBs, as can be noted by comparing the aggregation tendency of two series of compounds. All complexes of the **4a**−**c** series bear the *tert*-leucinate ligand, but the arene changes from benzene to hexamethylbenzene. This caused a dramatic decrease in the aggregation tendency that in **4a** (entries 11−16 in Table 2) was comparable to **1** and **2**, while substantially decreased in **4b** (entries 17−24 in Table 2) and still more in **4c** (entries 25, 26 in Table 2). In the second series, **1**, **2**, **4b**, **5**, and **6**, the arene was held constant, while the steric hindrance of the amino acidate ligand gradually increased. The aggregation tendency decreased as the steric hindrance increased: **1** (CH_2) ≈ **2** (CHMe) > **5** (CMe_2) ≈ **4b** (CH*t*-Bu) > **6** (CPh_2).

Another clear indication of the key role played by NH···X hydrogen bonds can be clearly seen by comparing the aggregation tendency of complexes **2**, **7**, and **3b**, which bear NH_2, NHR and NMe_2 moieties, respectively. Compound **2** showed a remarkable tendency to aggregate as described above. Complex **7**, which still has an N−H fragment, had a marked tendency to aggregate that was strongly dependent on which diastereoisomer was considered (*vide infra*); the maximum N value was 29.0 at 71.1 mM. Complex **3b**, which does not have an N−H moiety, showed a reduced tendency to aggregate ($N = 2.7$ at 114.4 mM).

The effect of changing the arene ligand in complexes **3a**−**c** was less important than in the **4a**−**c** series. While **3c** did not aggregate in $CDCl_3$, **3a** and **3b** showed a comparable aggregation tendency, and dimers appeared to be the predominant species. The latter probably formed as a consequence of aromatic C−H···X interactions[19] that may have been enforced by $\pi-\pi$ stacking interactions.

For complexes **2**, **4**, and **7**, mixtures of two diastereoisomers, which differed in the configuration on the metal center,[19] were observed in solution (Scheme 2). ^{1}H-PGSE measurements allowed the individual self-aggregation tendency of the two diastereoisomers to be evaluated. It was found that the two

Table 2. Diffusion Coefficients (D_t, m^2 s^{-1}), Hydrodynamic Radius (r_H, Å), Hydrodynamic Volume (V_H, Å^3), Aggregation Number (N), and Concentration (C, mM) for Compounds 1 and 3−7 in $CDCl_3$ (ϵ_r = 4.81 at 20 °C)

entry	compound	$10^{10} D_t$	r_H	V_H	N	C
1	**1**	5.75	7.1	1506	6.5	1.5[a]
2	**3a**	10.5	4.4	366	1.9	0.9
3	**3a**	9.5	4.7	440	2.2	4.7[a]
4	**3b**	8.93	4.9	478	1.9	1.8
5	**3b**	8.86	5.0	525	2.1	12.5
6	**3b**	8.74	4.9	502	2.0	18.6
7	**3b**	7.87	5.1	556	2.2	45.6
8	**3b**	7.40	5.2	596	2.4	58.1
9	**3b**	6.51	5.5	686	2.7	114.4
10	**3c**	10.2	4.2	317	1.1	0.5
11	(S_{Ru}, S_C)-**4a**	6.98	6.0	896	3.9	0.74
12	(S_{Ru}, S_C)-**4a**	4.18	9.3	3369	13.4	3.62
13	(S_{Ru}, S_C)-**4a**	2.79	13.3	9877	37.6	15.2
14	(R_{Ru}, S_C)-**4a**	6.86	6.1	928	4.0	0.46
15	(R_{Ru}, S_C)-**4a**	4.29	9.08	3136	12.6	2.33
16	(R_{Ru}, S_C)-**4a**	2.79	13.3	9877	37.6	9.4
17	(S_{Ru}, S_C)-**4b**	7.56	5.6	720	2.6	0.38
18	(S_{Ru}, S_C)-**4b**	7.60	5.7	768	2.8	1.37
19	(S_{Ru}, S_C)-**4b**	4.49	8.8	2806	9.5	6.2
20	(S_{Ru}, S_C)-**4b**	3.80	9.8	3990	13.1	10.5[a]
21	(R_{Ru}, S_C)-**4b**	7.91	5.4	649	2.3	0.32
22	(R_{Ru}, S_C)-**4b**	7.65	5.6	755	2.7	1.07
23	(R_{Ru}, S_C)-**4b**	4.71	8.4	2447	8.4	4.6
24	(R_{Ru}, S_C)-**4b**	4.01	9.3	3413	11.3	7.8[a]
25	(S_{Ru},S_C)-**4c**	11.7	4.8	463	1.5	0.9
26	(R_{Ru},S_C)-**4c**	11.7	4.8	463	1.5	0.8
27	**5**	8.37	5.2	582	2.3	1.6[a]
28	**6**	7.32	5.7	792	2.3	3.0
29	**6**	5.37	7.2	1557	4.4	21.0
30	**6**	3.22	10.2	4432	11.8	70
31	(S_{Ru}, S_N, S_C)-**7**	8.37	5.1	559	2.2	3.4
32	(S_{Ru}, S_N, S_C)-**7**	7.61	5.5	690	2.7	9.9
33	(S_{Ru}, S_N, S_C)-**7**	5.97	6.3	1068	4.1	34.4
34	(S_{Ru}, S_N, S_C)-**7**	4.59	7.5	1774	6.7	116
35	(S_{Ru}, S_N, S_C)-**7**	1.98	8.9	2903	10.6	178
36	(R_{Ru}, S_N, S_C)-**7**	7.70	5.4	663	2.6	1.4
37	(R_{Ru}, S_N, S_C)-**7**	7.54	5.5	702	2.8	3.9
38	(R_{Ru}, S_N, S_C)-**7**	4.05	8.9	2937	10.7	13.8
39	(R_{Ru}, S_N, S_C)-**7**	3.06	10.9	5407	19.0	46.6
40	(R_{Ru}, S_N, S_C)-**7**	1.36	12.6	8411	29.0	71.1

[a] Saturated solution.

Scheme 2

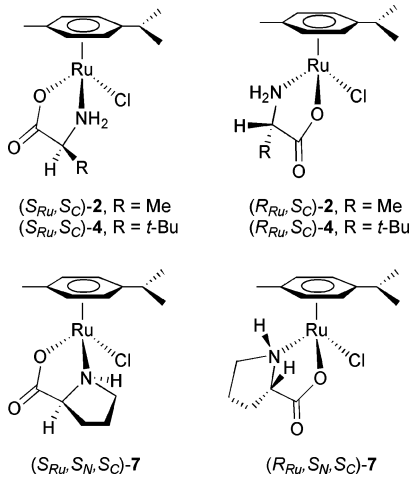

diastereoisomers of the complexes with the alaninate and *tert*-leucinate (**4b**) ligands (Scheme 2) showed substantially the same tendency to aggregate. In contrast, the least abundant diastereoisomer of the complexes with prolinate [(R_{Ru}, S_N, S_C)-**7**] showed a remarkably higher aggregation tendency than the other one [(S_{Ru}, S_N, S_C)-**7**] (Figure 3).

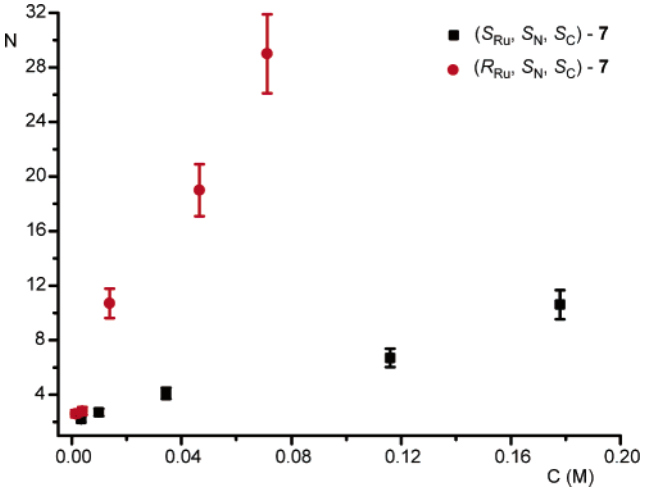

Figure 3. Dependence of the aggregation number (N) on the concentration (C) for the two diastereoisomers of **7** in $CDCl_3$.

A possible explanation for this differential tendency of the two diastereoisomers to aggregate can be found by looking at their structures (Scheme 2). In fact, in (S_{Ru}, S_N, S_C)-**7** the N−H bond is oriented toward the chlorine atom and an N−H···Cl−Ru intramolecular hydrogen bond can be established, making the N−H moiety less available for intermolecular interactions. Indeed, the N−H···Cl−Ru distance was found to be 2.83 Å in the solid-state structure of (S_{Ru},S_N,S_C)-[RuCl(Pro)(benzene)].[23] Instead, in the (R_{Ru}, S_N, S_C)-**7** diastereoisomer the N−H bond points toward the cymene and is prone to interact with oxygen or chlorine atoms of other complexes, forming intermolecular aggregates.

The marked difference in the aggregation tendency of the (S_{Ru},S_N,S_C)-**7** and (R_{Ru},S_N,S_C)-**7** diastereoisomers suggests that a diastereoisomeric recognition process takes place in solution that leads to the formation of homochiral adducts.[24] This does not seem to be the case for the (S_{Ru},S_C) and (R_{Ru},S_C) diastereoisomers of complexes with alaninate and *tert*-leucinate ligands, which showed the same tendency to self-aggregate. In agreement with these observations, the solid-state structures of Ru−arene complexes bearing the alaninate ligands contain both diastereoisomers,[20,21] while in the one with the prolinate ligand only one [(S_{Ru},S_N,S_C)] is present.[23] The configuration on the nitrogen that bears the functionality (N−H) is prevalently responsible for the formation of intermolecular adducts, in order to obtain diastereoselective self-aggregation and subsequent crystallization.[25]

Determination of the Thermodynamic Parameters of the Aggregation Process. The equilibrium constant (K) and, consequently, the standard variation of the free energy ($\Delta G°$) for the aggregation process were determined for complexes **2**, **3b**, **4b**, and **7** at 296 K. It was assumed that the aggregation process is well-described by the Equal K (EK) self-aggregation model.[26] Schematizing the self-aggregation process as

$$A_{n-1} + A = A_n$$

where A = [RuCl(AA)(Arene)] and $n \geq 2$, the EK model

(23) Kraemer, R.; Polborn, K.; Wanjek, H.; Zahn, I.; Beck, W. *Chem. Ber.* **1990**, *123*, 767.

(24) (a) Saraswathi, N. T.; Roy, S.; Vijayan, M. *Acta Crystallogr., Sect. B* **2003**, *59*, 641. (b) Harvey, N. G.; Rose, P. L.; Mirajovsky, D.; Arnett, E. M. *J. Am. Chem. Soc.* **1990**, *112*, 3547. (c) Okabayashi, H. F.; Makoto, I.; O'Connor, C. J. *Self-Assembly*; Robinson, B. H., Ed.; IOS Press: Amsterdam, 2003. (d) Hoffmann, F.; Stine, K. J.; Hühnerfuss, H. *J. Phys. Chem. B* **2005**, *109*, 240.

(25) Cooks, R. G.; Zhang, D.; Koch, K. J. *Anal. Chem.* **2001**, *73*, 3646.

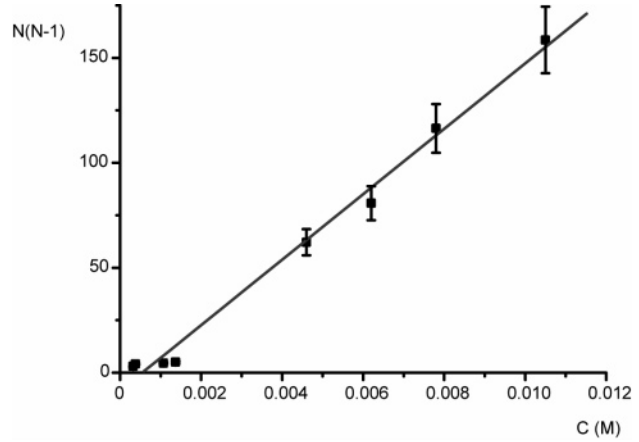

Figure 4. Dependence of $N(N-1)$ on the concentration for complex **4b** in $CDCl_3$.

Table 3. Equilibrium Constants (K) and Free Energies of the Aggregation Process ($\Delta G°$) for Compounds 2, 3b, 4b, 5, and 7 in Different Solvents

entry	compound	solvent (ϵ at 25 °C)	10^{-2} K (M^{-1})	$-\Delta G°$ (kcal mol^{-1})
1	**2**	$CDCl_3$ (4.81[a])	1700 ± 170	7.1 ± 0.7
2	**2**	CD_2Cl_2 (8.93)	145 ± 14	5.6 ± 0.6
3	**2**	acetone-d_6 (20.56)	7.8 ± 0.8	3.9 ± 0.4
4	**2**	2-propanol-d_8 (19.92)	1.7 ± 0.2	3.0 ± 0.3
5	**3b**	$CDCl_3$ (4.81[a])	0.25 ± 0.02	1.9 ± 0.2
6	**4b**	$CDCl_3$ (4.81[a])	156 ± 16	5.7 ± 0.6
7	(S_{Ru}, S_N, S_C)-**7**	$CDCl_3$ (4.81[a])	3.2 ± 0.3	3.4 ± 0.3
8	(R_{Ru}, S_N, S_C)-**7**	$CDCl_3$ (4.81[a])	76 ± 8	5.2 ± 0.5

[a] ϵ_r at 20 °C.

assumes that (a) the entropy change of the equilibrium reactions is constant and (b) the enthalpy change is independent of the value of n. Under these assumptions, a single K describes the system, and the concentration (C) can be written as

$$C = [A] + 2[A_2] + ... + i[A_i] + ... = [A]/(1 - K[A])^2 \quad (1)$$

while the total concentration of aggregates (C_A) can be written as

$$C_A = [A] + [A_2] + ... + [A_i] + ... = [A]/(1 - K[A]) \quad (2)$$

The aggregation number N can be expressed as the ratio C/C_A. By combining this definition of N with eqs 1 and 2 the following equation is obtained:

$$N(N-1) = KC \quad (3)$$

Plotting $N(N-1)$, derived from PGSE NMR measurements, versus C led to linear trends that were fitted with eq 3. Values of the equilibrium constant were obtained from the slope of the linear fit (Figure 4) (Supporting Information). Table 3 summarizes the results of the fits for different complexes. $\Delta G°$ was estimated from the K values (Table 3).

A comparison between the $\Delta G°$ values for **2** and **3b** in $CDCl_3$ (entries 1 and 5 in Table 3) allows the weight of the hydrogen bonding involving the NH_2 moiety to be determined. $|\Delta(\Delta G°)|$ is equal to 5.3 kcal/mol and is consistent with the energy of two "classical" HBs in chloroform.[27,28] $\Delta G°$ for the aggregation of the (S_{Ru}, S_N, S_C)-**7** and (R_{Ru}, S_N, S_C)-**7** diastereoisomers (−3.4 and −5.2 kcal/mol, respectively) are rather different and reflect their above-mentioned markedly different tendency to self-aggregate.[29] A more incisive consideration can be done by comparing the $\Delta G°$ of (S_{Ru}, S_N, S_C)-**7** and (R_{Ru}, S_N, S_C)-**7** with that of **2**. The substitution of the H atom of the NH_2 moiety pointing toward cymene with the aliphatic chain of the proline ring, i.e., passing from **2** to (S_{Ru}, S_N, S_C)-**7**, leads to a $|\Delta(\Delta G°)|$ of 3.7 kcal/mol. The substitution of the other NH_2 proton that points toward the chlorine, i.e., passing from **2** to (R_{Ru}, S_N, S_C)-**7**, has a minor effect on the aggregation, leading to a $|\Delta(\Delta G°)|$ of 1.9 kcal/mol. Finally, the $|\Delta(\Delta G°)|$ of 1.4 kcal/mol between **2** and **4b**, which both bear the NH_2 moiety, indicates that steric effects can also play an important role.

The aggregation tendency of complex **2** was investigated in $CDCl_3$, CD_2Cl_2, acetone-d_6, and 2-propanol-d_8. The K and $\Delta G°$ values reported in Table 3 clearly indicate that aggregation is favored by a reduction of the relative permittivity of the solvent. For the three aprotic solvents taken into account the following trend was obtained for $-\Delta G°$(kcal/mol): 7.1 in $CDCl_3$ (ϵ_r = 4.81) > 5.6 in CD_2Cl_2 (ϵ_r = 8.93) > 3.9 in acetone-d_6 (ϵ_r = 20.56). This is in line with the fact that the main aggregation motif is hydrogen bonding, which is known to be disfavored by an increase in the solvent polarity.[30] The observed decrease of the $\Delta G°$ passing from acetone-d_6 ($\Delta G°$ = 3.9 kcal/mol, ϵ_r = 20.56) to 2-propanol-d_8 ($\Delta G°$ = 3.0 kcal/mol, ϵ_r = 19.92), which have almost the same polarity, is perfectly reasonable considering that the protic nature of the latter solvent makes it suitable to undergo hydrogen bonding with a half-sandwich amino acidate unit providing those functionalities that are responsible for aggregation.

Conclusions

The intermolecular interactions responsible for the self-aggregation of [RuCl(AA)(Arene)] complexes were identified and quantified through ^1H diffusion NMR measurements by varying the properties of ligands and solvent. The complexes showed a remarkable tendency to self-aggregate, forming nanosized adducts under favorable conditions (solvents with low relative permittivity, elevated concentration, little encumbered ligands). A key role was played by the N−H functionality of AA that allowed the establishment of intermolecular H-bonds. When N−H was present, dimers (or higher aggregates) were always predominant even at the lowest investigated concentration. The orientation of the N−H moiety also appeared to be important and led to an interesting diastereoisomeric intermolecular recognition process. This was clearly shown by the different self-aggregation tendency of the two diastereoisomers (S_{Ru},S_N,S_C)-[RuCl(Pro)(*p*-cymene)] and (R_{Ru},S_N,S_C)-[RuCl(Pro)(*p*-cymene)]. In addition, the former, having the N−H moiety engaged in an intramolecular H-bond with the chloride, showed a significantly smaller tendency to self-aggregate than the latter.

Experimental Section

All reagents were purchased from Sigma-Aldrich and used without any further purification. $[Ru(\eta^6\text{-arene})_2Cl_2]_2$ was prepared

(26) (a) Ts'O, P. O. P.; Melvin, I. S.; Olson, A. C. *J. Am. Chem. Soc.* **1963**, *85*, 1289. (b) Martin, R. B. *Chem. Rev.* **1996**, *96*, 3043, and references therein.

(27) Rivas, J. C. M.; Salvagni, E.; de Rosales, R. T. M. *Dalton Trans.* **2003**, *17*, 3339.

(28) Yajima, T.; Maccarrone, G.; Takani, M.; Contino, A.; Arena, G.; Takamido, R.; Hanaki, M.; Funahashi, Y.; Odani, A.; Yamauchi, O. *Chem.−Eur. J.* **2003**, *9*, 3341.

(29) Hünenberger, P. H.; Granwehr, J. K.; Aebischer, J.-N.; Ghoneim, N.; Haselbach, E.; van Gunsteren, W. F. *J. Am. Chem. Soc.* **1997**, *119*, 7533.

(30) Reichardt, C. *Solvents and Solvent Effect in Organic Chemistry*; Wiley-VCH: Weinheim, 2003.

according to Bennett et al.[31] Compounds **1**−**7** were synthesized according to the literature,[32] using the standard Schlenk technique, and fully characterized through one- and two-dimensional NMR techniques. Solvents were freshly distilled (*n*-hexane with Na, Et_2O with Na/benzophenone, MeOH with CaH_2, CH_2Cl_2 with P_2O_5) and degassed, by many gas−pump−nitrogen cycles before use.

All complexes were characterized through ^{1}H, ^{13}C, ^{1}H−COSY, ^{1}H-NOESY, ^{1}H,^{13}C-HMQC NMR, and ^{1}H,^{13}C-HMBC NMR experiments recorded on a Bruker DRX 400 spectrometer. Referencing was relative to TMS. NMR samples were prepared by dissolving a suitable amount of compound in 0.5 mL of solvent.

Synthesis of Complex 1. $[RuCl_2(p\text{-cymene})]_2$ (0.100 g, 0.163 mmol), glycine (0.0244 g, 0.326 mmol), and potassium *tert*-butoxide (0.0365 g, 0.326 mmol) were dissolved in the minimal amount of methanol and stirred for 30 min. The volume of the deep red solution was reduced, and dichloromethane was added. Potassium chloride precipitated and was filtered off. Addition of diethyl ether to the red solution caused the precipitation of the desired product. The latter was filtered and dried under vacuum to give an orange solid, which was stored under nitrogen. Yield: 70%. ^{1}H NMR (2-propanol-d_8, 298 K, 400.13 MHz, *J* in Hz): δ 6.45 (m, 1H, N*H*), 5.70 (d, 1H, ^3J = 5.4), 5.65 (d, 1H, ^3J = 5.6), 5.51 (d, 1H, ^3J = 5.7), 5.45 (d, 1H, ^3J = 5.5), 4.03 (m, 1H, N*H*), 3.08 (m, 2H, 8), 2.94 (sept, 1H, $^3J_{6-7}$ = 6.8, H6), 2.23 (s, 3H, H1), 1.35 (m, 6H, H7). Anal. Calcd for $C_{12}H_{22}ClNO_2Ru$: C, 41.80; H, 5.60; N, 4.06. Found: C, 40.9; H, 5.8; N, 3.9.

Synthesis of Complex 2. The procedure was equivalent to that described for complex **1**. Yield: 75%. ^{1}H NMR ($CDCl_3$, 298 K,

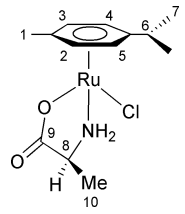

400.13 MHz, *J* in Hz), (S_{Ru}, S_C)-**2**: δ 7.63 (m, 1H, N*H*), 5.73 (m, 2.4H), 5.60 (d, 1H, $^3J_{H3-H4}$ = 5.6, H3), 5.52 (m, 2.7H), 3.50 (m, 1H, H8), 2.90 (m, 1.7H, H6), 2.52 (m, 1H, N*H*), 2.21 (s, 3H, H10), 1.43 (d, 3H, $^3J_{H7-H6}$ = 6.7, H7), 1.33 (m, 10.2H). ^{13}C{^{1}H} NMR ($CDCl_3$, 298 K, 100.55 MHz): δ 182.5 (C9), 101.4 (C2), 96.1 (C5), 82.8 (C4), 81.2 (C3), 81.1 (C3), 80.5 (C4), 53.4 (C8), 31.4 (C6), 23.3 (C7), 18.8 (C10). ^{1}H NMR ($CDCl_3$, 298 K, 400.13 MHz, *J* in Hz), (R_{Ru}, S_C)-**2**: δ 5.95 (m, 0.7H, N*H*), 5.73 (m, 2.4H), 5.67 (d, 0.7H, $^3J_{H3-H4}$ = 5.2, H4), 5.52 (m, 2.7H), 3.69 (m, 0.7H, N*H*), 3.30(m, 0.7H, H8), 2.90 (m, 1.7H, H6), 2.24 (s, 2.1H, H10), 1.47 (d, 2.1H, $^3J_{H7-H6}$ = 6.7, H7), 1.33 (m, 10.2H). ^{13}C{^{1}H} NMR ($CDCl_3$, 298 K, 100.55 MHz): δ 183.9 (C9), 101.3 (C2), 96.4 (C5), 83.1 (C4), 82.7 (C3), 81.0 (C3), 82.2 (C4), 51.8 (C8), 31.4 (C6), 21.6 (C7), 19.9 (C7), 18.7 (C10).

Synthesis of Complex 3a. $[RuCl_2(benzene)]_2$ (0.100 g, 0.200 mmol), *N*,*N*-dimethylglycine (0.0412 g, 0.400 mmol), and potassium *tert*-butoxide (0.0448 g, 0.400 mmol) were dissolved in the minimal amount of methanol and stirred for 30 min. The volume of the deep red solution was reduced, and dichloromethane was added. Potassium chloride precipitated and was filtered off. Addition of diethyl ether to the red solution caused the precipitation of the desired product. The latter was filtered and dried under vacuum to give an orange solid, which was stored under nitrogen. Yield: 58%. ^{1}H NMR ($CDCl_3$, 298 K, 400.13 MHz, *J* in Hz): δ 5.40 (s, 6H, C_6H_6), 3.32 (d, 1H, ^2J = 14.6 Hz, H8), 2.96 (s, 3H, N*Me*), 2,75 (s, 3H, N*Me*), 2.18 (d, 1H, ^2J = 14.8 Hz, H8). Anal. Calcd for $C_{10}H_{14}ClNO_2Ru$: C, 37.92; H, 4.46; N, 4.42. Found: C, 38.0; H, 4.8; N, 4.1.

Synthesis of Complex 3b. The procedure was equivalent to that described for complex **1**. Yield: 61%. ^{1}H NMR ($CDCl_3$, 298 K, 400.13 MHz, *J* in Hz): δ 5.41 (d, 1H, ^3J = 5.9 Hz, H2), 5.38 (m, 2H), 5.33 (d, 1H, ^3J = 6.0 Hz), 3.58 (d, 1H, ^2J = 14.6 Hz, H8), 4.04 (m, 1H, N*H*), 3.14 (s, 3H, N*Me*$_2$), 3.00 (sept, 1H, ^3J = 7.0 Hz, H6), 2.92 (s, 3H, N*Me*$_2$), 2.43 (d, 1H, ^2J = 14.8 Hz, H8), 2.27 (s, 3H, H1), 1.36 (m, 6H, H7). Anal. Calcd for $C_{14}H_{22}ClNO_2Ru$: C, 45.10; H, 5.95; N, 3.76. Found: C, 46.3; H, 6.3; N, 3.5.

Synthesis of Complex 3c. $[RuCl_2(hexamethylbenzene)]_2$ (0.100 g, 0.150 mmol), glycine (0.0309 g, 0.300 mmol), and potassium *tert*-butoxide (0.0337 g, 0.300 mmol) were dissolved in the minimal amount of methanol and stirred for 30 min. The volume of the deep red solution was reduced, and dichloromethane was added. Potassium chloride precipitated and was filtered off. Addition of diethyl ether to the red solution caused the precipitation of the desired product. The latter was filtered and dried under vacuum to give an orange solid, which was stored under nitrogen. Yield: 70%. ^{1}H NMR (CD_2Cl_2, 298 K, 400.13 MHz, *J* in Hz): δ 3.47 (d, 1H, ^2J = 14.4, H8), 2.90 (s, 3H, N*Me*$_2$), 2.72 (s, 3H, N*Me*$_2$), 2.28 (d, ^2J = 14.8, H8), 2.12 (s, 18H, C_6Me_6). Anal. Calcd for $C_{16}H_{26}ClNO_2Ru$: C, 47.93; H, 6.54; N, 3.49. Found: C, 46.5; H, 7.0; N, 3.6.

Synthesis of Complex 4a. The procedure was equivalent to that described for complex **3a**. Yield: 80%. ^{1}H NMR (acetone-d_6, 298 K, 400.13 MHz, *J* in Hz) (S_{Ru}, S_C)-**4a**: δ 6.87 (m, 1H, N*H*), 5.71 (s, 6H, C_6H_6), 3.05 (d, ^3J = 6.5, 1H, H8), 2.54 (m, 1H, N*H*), 1.04 (s, 9H, Bu^t). ^{1}H NMR (acetone-d_6, 298 K, 400.13 MHz, *J* in Hz) (R_{Ru}, S_C)-**4a**: δ 5.69 (s, 2H, C_6H_6), 5.60 (m, 0.3H, N*H*), 4.46 (m, 0.3H, N*H*), 3.08 (d, ^3J = 6.4, 0.3H, H8), 1.09 (s, 3H, Bu^t). Anal. Calcd for $C_{12}H_{18}ClNO_2Ru$: C, 41.80; H, 5.26; N, 4.06. Found: C, 42.3; H, 5.8; N, 3.8.

Synthesis of Complex 4b. The procedure was equivalent to that described for complex **1**. Yield: 75%. ^{1}H NMR (2-propanol-d_8, 298 K, 400.13 MHz, *J* in Hz) (S_{Ru}, S_C)-**4b**: δ 7.01 (m, 1H, N*H*), 5.73 (d, 1H, ^3J = 6.0, H3), 5.62 (d, 1H, ^3J = 5.8, H2), 5.59 (d, 1H, ^3J = 5.8, H4), 5.47 (m, 1.7H), 3.00 (dd, 1H, ^3J = 6.6, ^3J = 11.3, H8), 2.88 (m, 3.2H), 2.24 (s, 3H, H1), 1.32 (m, 8.4H), 1.13 (s, 9H, Bu^t); (R_{Ru}, S_C)-**4b**: δ 5.71 (d, 0.7H, ^3J = 5.6, H3), 5.66 (d, ^3J = 5.9, H3), 5.55 (d, 0.7H, ^3J = 5.5, H4), 5.47 (m, 1.7H), 5.24 (m, 0.7H, N*H*), 2.88 (m, 3.2H), 2.25 (s, 1.8H, H1), 1.32 (m, 8.4H), 1.15 (s, 5.4H, Bu^t).

Synthesis of Complex 4c. The procedure was equivalent to that described for complex **3c**. Yield: 82%. ^{1}H NMR (2-propanol-d_8, 298 K, 400.13 MHz, *J* in Hz) (S_{Ru}, S_C)-**4c**: δ 6.53 (m, 1H, N*H*), 3.15 (m, 1.5H), 2.88 (m, 1H, N*H*), 2.10 (s, 18H, C_6Me_6). ^{1}H NMR (2-propanol-d_6, 298 K, 400.13 MHz, *J* in Hz) (R_{Ru}, S_C)-**4c**: δ 4.40 (m, 0.5H, N*H*), 3.88 (m, 0.5H, N*H*), 3.15 (m, 1.5H), 2.21 (s, 6H, C_6Me_6). Anal. Calcd for $C_{18}H_{30}ClNO_2Ru$: C, 50.40; H, 7.05; N, 3.27. Found: C, 51.9; H, 8.0; N, 2.9.

Synthesis of Complex 5. The procedure was equivalent to that described for complex **1**. Yield: 66%. ^{1}H NMR (2-propanol-d_8, 298 K, 400.13 MHz, *J* in Hz): δ 5.69 (d, 1H, ^3J = 5.7), 5.65 (m, 1H, N*H*), 5.62 (d, 1H, ^3J = 6.0), 5.51 (d, 1H, ^3J = 5.7), 5.42 (d, 1H, ^3J = 5.8), 3.45 (m, 1H, H8), 3.14 (d, 1H, ^2J = 10.6 Hz, N*H*), 2.89 (sept, 1H, ^3J = 6.9 Hz, H6), 2.21 (s, 3H, H1), 1.42 (s, 3H, H10), 1.38 (s, 3H, H10), 1.34 (d, 3H, ^3J = 6.8 Hz, H7), 1.33(d, 3H, ^3J = 6.9 Hz, H7). Anal. Calcd for $C_{14}H_{22}ClNO_2Ru$: C, 45.10; H, 5.95; N, 3.76. Found: C, 47.1; H, 5.8; N, 3.95.

Synthesis of Complex 6. The procedure was equivalent to that described for complex **1**. Yield: 88%. ^{1}H NMR ($CDCl_3$, 298 K, 400.13 MHz, *J* in Hz): δ 7.76 (m, 2H), 7.48 (m, 3H), 7.10 (m, 3H), 6.99 (m, 2H), 5.36 (d, 1H, ^3J = 6.5 Hz), 5.15 (m, 2H), 4.73 (d, 1H, ^3J = 6.5 Hz), 3.99 (d, 1H, ^2J = 10.6 Hz, N*H*), 2.49 (m, 1H, 6), 1.90 (m, 1H, N*H*), 1.64 (s, 3H, H1), 1.11 (d, 3H, ^3J = 6.2

(31) Bennett, M. A.; Huang, T. N.; Matheson, T. W.; Smith, A. K. *Inorg. Synth.* **1982**, *21*, 74.

(32) (a) Dersnah, D. F.; Baird, M. C. *J.Organomet. Chem.* **1977**, *127*, C55−C58. (b) Sheldrick, W. S.; Heeb, S. *Inorg. Chim. Acta* **1990**, *168*, 93.

Hz, H7), 1.07 (d, 3H, ^3J = 6.2 Hz, H7). Anal. Calcd for $C_{12}H_{22}ClNO_2Ru$: C, 41.80; H, 5.60; N, 4.06. Found: C, 40.9; H, 5.8; N, 3.9.

Synthesis of Complex 7. The procedure was equivalent to that described for complex **1**. ^{1}H NMR (CD_2Cl_2, 298 K, 400.13 MHz, *J* in Hz) (S_{Ru}, S_C, S_N)-**7**: δ 5.54 (m, 1.68H), 5.43 (m, 2H), 5.25 (d, 1H, ^3J = 5.7), 4.08 (m, 1H, N*H*), 3.90 (m, 1H), 3.52 (dd, $^3J_{8-NH}$ = 17.7, $^3J_{8-10}$ = 8.7, H8), 3.12 (m, 1H), 2.88 (m, 1.34H), 2.23 (s, 3H, H1), 1.86 (m, 1.7H), 1.78 (m, 2.34H), 1.34 (m, 8H); (R_{Ru}, S_C, S_N)-**7**: δ 8.00 (m, 0.34H, N*H*), 5.71 (d, 0.34H, ^3J = 5.7), 5.63 (d, 0.34H, ^3J = 5.5), 5.54 (m, 1.68H), 3.75 (m, 0.34H), 3.41 (m, 0.34H), 3.29 (m, 0.34H), 2.88 (m, 1.34H), 2.20 (s, 1H, H1), 1.86 (m, 1.7H), 1.78 (m, 2.34H), 1.34 (m, 8H).

NOE Measurements. The ^{1}H-NOESY[33] NMR spectra were acquired by the standard three-pulse sequence or by the PFG version.[34] The number of transients and the number of data points were chosen according to the sample concentration and the desired final digital resolution. Semiquantitative spectra were acquired using a 1 s relaxation delay and 800 ms mixing times. Quantitative ^{1}H-NOESY NMR experiments were carried out with a relaxation delay of 10 s.

PGSE NMR Measurements. ^{1}H NMR measurements were performed by using the standard stimulated echo pulse sequence[11] on a Bruker AVANCE DRX 400 spectrometer equipped with a GREAT 1/10 gradient unit and a QNP probe with a Z-gradient coil, at 296 K without spinning. The shape of the gradients was rectangular, their duration (δ) was 4−5 ms, and their strength (*G*) was varied during the experiments. All of the spectra were acquired using 32K points and a spectral width of 5000 (^{1}H) Hz and processed with a line broadening of 1.0 (^{1}H) Hz. The semilogarithmic plots of $\ln(I/I_0)$ versus G^2 were fitted using a standard linear regression algorithm; the *R* factor was always higher than 0.99. Different values of Δ, "nt" (number of transients), and number of different gradient strengths (*G*) were used for different samples. The methodology for treating data was described previously.[18] All van der Waals volumes was computed from the crystal structures using the WebLab ViewerLite 4.0 software packages. The uncertainity in the measurements was estimated by determining the standard deviation of the slopes of the linear regression lines by performing experiments with different Δ values. The standard propagation of error analysis gave a standard deviation of approximately 3−4% in hydrodynamic radii and 10−15% in hydrodynamic volumes and aggregation numbers *N*.

Evaluation of *N* for Large Aggregates. *N* was calculated by the $[(V_H - V_{INT})/V_{vdW}]$ ratio, where V_{INT} represents the interstitial volume. It was assumed that molecules had a spherical shape and a face-centered cubic package. Under these assumptions the packing density (*P*) ($V_{occupied}/V_{total}$) is 0.7405 for an infinite lattice and there are *N* "octahedral" (O_{cav}) and 2*N* "tetrahedral" (T_{cav}) cavities in the cell.[35] While it is not possible to calculate the volume of these cavities separately, the radius of the largest sphere that can fill the two types of cavities (r_{Ocav}, r_{Tcav}) is known.[35] From these radii we deduced the edge and volume of the octahedron (O_{insc}) and tetrahedron (T_{insc}) inscribed in the respective spheres. Finally, we assumed that the ratio $V(T_{insc})/V(O_{insc})$ (0.3210) was equal to the ratio $V(T_{cav})/V(O_{cav})$. Since $P = 0.7405 = NV_{vdW}/[NV_{vdW} + NV(O_{cav}) + 2NV(T_{cav})] = V_{vdW}/[V_{vdW} + 1.6420V(O_{cav})]$, it was calculated that $V(O_{cav}) = 0.2134V_{vdW}$ and $V(T_{cav}) = 0.06850V_{vdW}$. *N* was estimated by knowing $V(O_{cav})$ and $V(T_{cav})$ and by evaluating the number of cavities through models.

Acknowledgment. We thank the Ministero dell'Istruzione, dell'Università e della Ricerca (MIUR, Rome, Italy), Programma di Rilevante Interesse Nazionale, Cofinanziamento 2004−2005 for support.

Supporting Information Available: ^{1}H NMR spectra of new compounds, complete data of PGSE NMR measurements (Table S1), and dependence of $N(N - 1)$ on the concentration for complexes **2** (Figures S1−S4), **3b** (Figure S5), **4b** (Figure S6), **5** (Figure S7), (S_{Ru}, S_N, S_C)-**7** (Figure S8), and (R_{Ru}, S_N, S_C)-**7** (Figure S9). This material is available free of charge via the Internet at http://pubs.acs.org.

OM060904E

(33) Jeener, J.; Meier, B. H.; Bachmann, P.; Ernst, R. R. *J. Chem. Phys.* **1979**, *71*, 4546.
(34) Wagner, R.; Berger, S. *J. Magn. Reson. A* **1996**, *123*, 119.
(35) West, A. *Solid State Chemistry and Its Applications*; John Wiley & Sons: New York, 1984.